Leslie A. Melim, James Hunter, and Mark Minton. Torosites: A New Microbially Mediated Speleothem from Sistema los Toros, Nuevo Léon, Mexico. *Journal of Cave and Karst Studies*, v. 86, nos. 1/2, p. 1-12. DOI:10.4311/2022ES0115

TOROSITES: A NEW MICROBIALLY MEDIATED SPELEOTHEM FROM SISTEMA LOS TOROS, NUEVO LÉON, MEXICO

Leslie A. Melim,[1,C] James Hunter,[2] and Mark Minton[3]

Abstract

Although several kinds of speleothems are known to grow with pendant morphology (i.e., helictites, pool fingers, and stalactites), we describe here a new form found in Sistema Los Toros, Nuevo Léon, Mexico, which we propose to call torosites. A laminated, bladed, spar crust grew beneath remnants of a stromatolitic micritic crust and extended mostly downward as irregular finger-like protrusions (torosites) that are 2–3 mm wide and 2–3 cm long. Although mainly pendants, the individual torosites are quite irregular with growth sideways and even upward in places. The torosites thicken and thin, like knuckles on a finger, but maintain a relatively uniform diameter. Laminations in the bladed spar and protrusions are defined by micritic intervals with minor intermixed detrital grains (clay, quartz, and carbonate silt) and rare, ropy biofilm. Bladed-spar crystals nucleate off thicker detrital layers, but they extend through thinner lamina. The torosites lack the central canal of helictites and most stalactites. Unlike pool fingers and stalactites, torosites only grow on the end of the speleothem, not on the sides. We hypothesize that the torosites grew from dripping water at their ends. Microbial biofilm communities colonized the growth surface, probably during drier conditions, forming the micritic layers. We speculate that the microbial mat likely caused the irregular sideways growth, but we cannot identify how on these fossil forms. Torosites are unique and add to the growing list of known microbially mediated speleothems.

INTRODUCTION

A location in Sistema Los Toros, Nuevo Léon, Mexico, contains a crust, now mostly eroded, with irregular finger-like protrusions extending down from the base and edges of that crust (Fig. 1). These protruding speleothems are unlike any previously described. This study describes the crust and the protruding speleothems and compares them with known pendant speleothems including pool fingers, subaqueous helictites, and stalactites. We propose the name torosites for these unique features and provide evidence their growth was microbially mediated.

METHODS

Three samples were collected for analysis from already broken pieces, including a piece of the crust and two fragments of the finger-like protrusions under the crust. Since the finger-like samples were so small (the larger was 2 mm × 10 mm), they were first vacuum embedded in epoxy. The resulting epoxy block was then cut and ground to reveal the center of the fingers, which allowed the thin section to bisect the two small fingers. The crust was also embedded in epoxy before slicing to retain loose material.

For scanning electron microscopy (SEM), either the thin section (fingers) or the thin section blank (crust) was first polished to remove any grinding grooves, and then etched in dilute hydrochloric acid for 10 seconds before rinsing in distilled water (after Melim et al., 2016). This etching process reveals insoluble components embedded in the carbonate and highlights subtle features (Melim and Spilde, 2021). A photomosaic of each thin section was constructed to guide navigation in the SEM. Dimensions were measured using ImageJ software version 1.53k (National Institutes of Health, 2021). The photomosaic combined with precise measurements allowed submicroscopic SEM fabrics to be matched with petrographic fabrics. SEM data were collected using a Tescan Vega 3 SEM at Western Illinois University with a Thermo Scientific UltraDry EDS (energy-dispersive spectroscopy) detector using Pathfinder X-ray Microanalysis System 1.3. All SEM samples were coated with gold-palladium. Operating conditions were an accelerating voltage of 15.0 kV and a beam intensity setting of 10.0.

RESULTS

Field Relationships

Three distinct components are present (Figs. 1–4): an upper-laminated crust, pale-tan in hand sample; a lower-bladed, calcite-spar crust, red-brown in the field (including the finger-like protrusions); and clastic sediments including carbonate silt, quartz silt, and clays.

The tan crust is above and to one side of a small pool and appears to have originally grown attached to the cave wall and cave floor (Fig. 1). It is now eroded into two distinct layers separated by a gap of several centimeters. The upper

[1] Department of Earth, Atmospheric, and Geographic Information Sciences, Western Illinois University, 1 University Cir., Macomb, IL 61455
[2] 223 Rio Bravo Dr., White Rock, NM 87547
[3] 8758 Frog Hollow Rd., Linville, VA 22834
[C] Corresponding Author: LA-Melim@wiu.edu

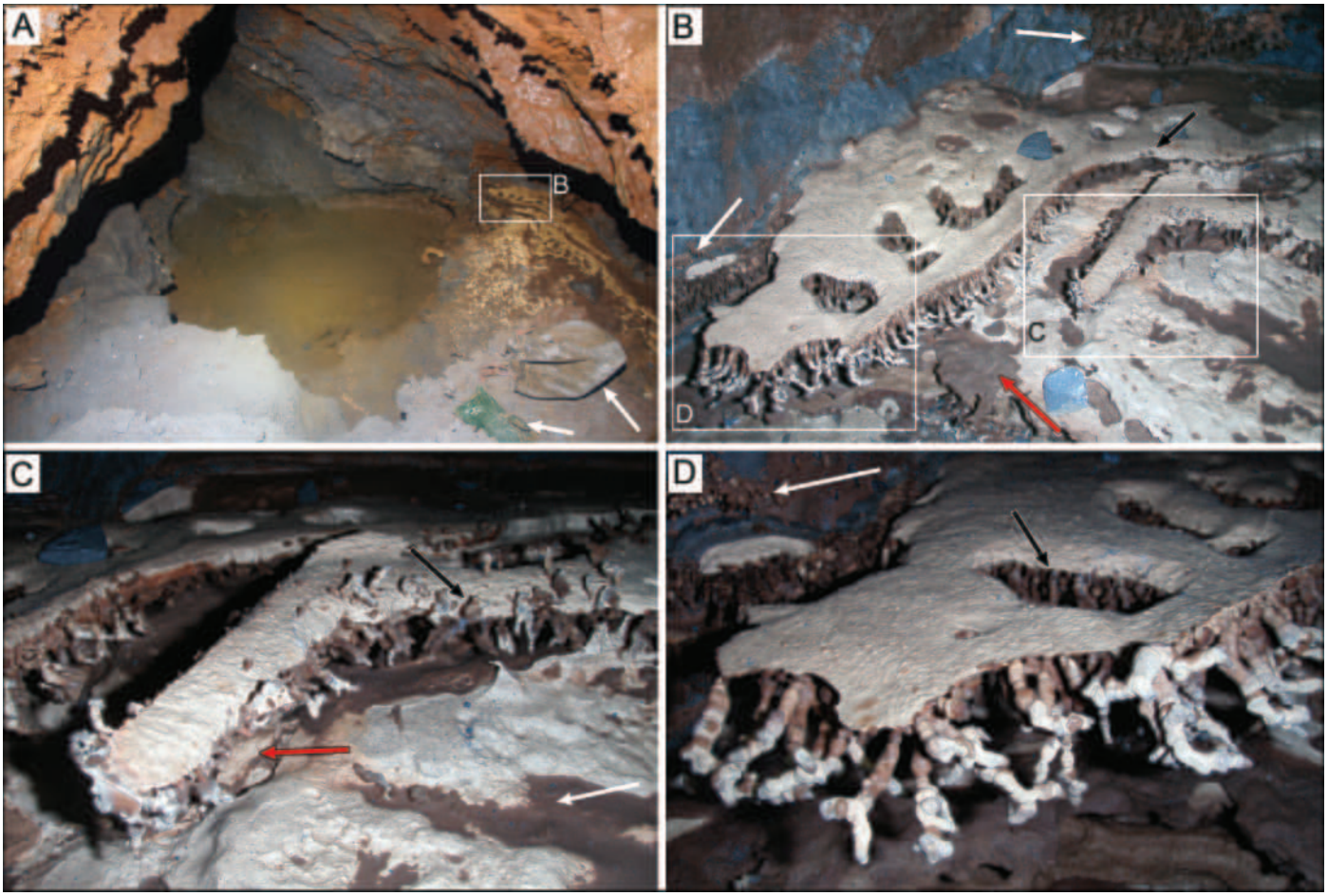

Figure 1. Photographs of crust and finger-like speleothems in Sistema Los Toros taken in December 2009 (A) and December 2008 (B, C, and D). Photos by James Hunter (A) and Aaron Moses (B, C, and D). A: Room shot of research site showing partly eroded crust next to a small pool. The cave bedrock is grey but there is red sediment coating parts of the walls and the crust suggesting flowing water in the near past. Note cave pack and gloves for scale (arrows). Box labeled B indicates location of Fig. 1B. B: Closer view of crust and finger-like speleothems. Light tan crust is eroded with irregular holes. Red sediment covers portions of the crust. The finger-like speleothems mostly extend down from the crust but also occur above the crust along the wall (white arrows) and rarely on eroded sides of the crust (black arrow). Those seen along the wall and through holes in the crust are smaller, darker, and closer to vertical. Those that occur on the edge of the crust extend sideways more and change color from dark red to white. A dark red crust, same color as fingers, is visible where the light tan crust has eroded away (red arrow). Boxes labeled C and D indicate closer views in Fig. 1C and 1D. C: Another view of the crust showing the two portions divided by a gap (red arrow). The upper portion crust is eroded with many holes. Note laminations in upper tan crust (black arrow) and modern red sediment (white arrow). Finger-like speleothems are visible though most of the holes in the crust. D: Detail on finger-like speleothems from Fig. 1B. The largest and most complex finger-like speleothems extend down and out from the edge of the eroded tan crust. These range from light red to white and bend and twist, with some branching. The diameter increases and decreases but remains about the same. Dark red examples are visible extending down from the interior of the crust (black arrow) and from the wall above the crust (white arrow).

portion extends out 10–20 cm from the wall as a shelf with peninsulas and irregular holes (Fig. 1A, 1B, and 1C). The lower portion coats the floor of the cave and has an irregular eroded top (Fig. 1C).

Growing mostly from base of the upper shelf is a second red crust with irregular, finger-like protrusions that are 2–3 mm wide and 2–3 cm long (Figs, 2, 3, and 4). Although generally extending down, the finger-like protrusions on the outer edge go sideways, sometimes branch, and rarely extend slightly upward (Fig. 1D). Although each protrusion tapers at the end, the thickness increases and decreases by ±0.2 mm, giving them a swollen-knuckle-like appearance (Figs. 3 and 4). Smaller examples also extend out from the eroded side of the crust (Fig. 1C) and down from the wall above the crust (Fig. 1B and 1D). The largest finger-like protrusions have white on the ends, but mostly they are red. Usually each protrusion extends directly from the tan crust, but some areas have a red sediment layer in between (Fig. 2).

Petrographic and SEM Observations

Upper Laminated Micritic Crust

The upper crust is laminated micrite with domed growth lines (Fig. 2). The laminae alternate between 10–20 µm thick micritic and 20–100 µm thick microspar layers (Figs. 2, 5A, and 5B). Most layers are continuous across the entire

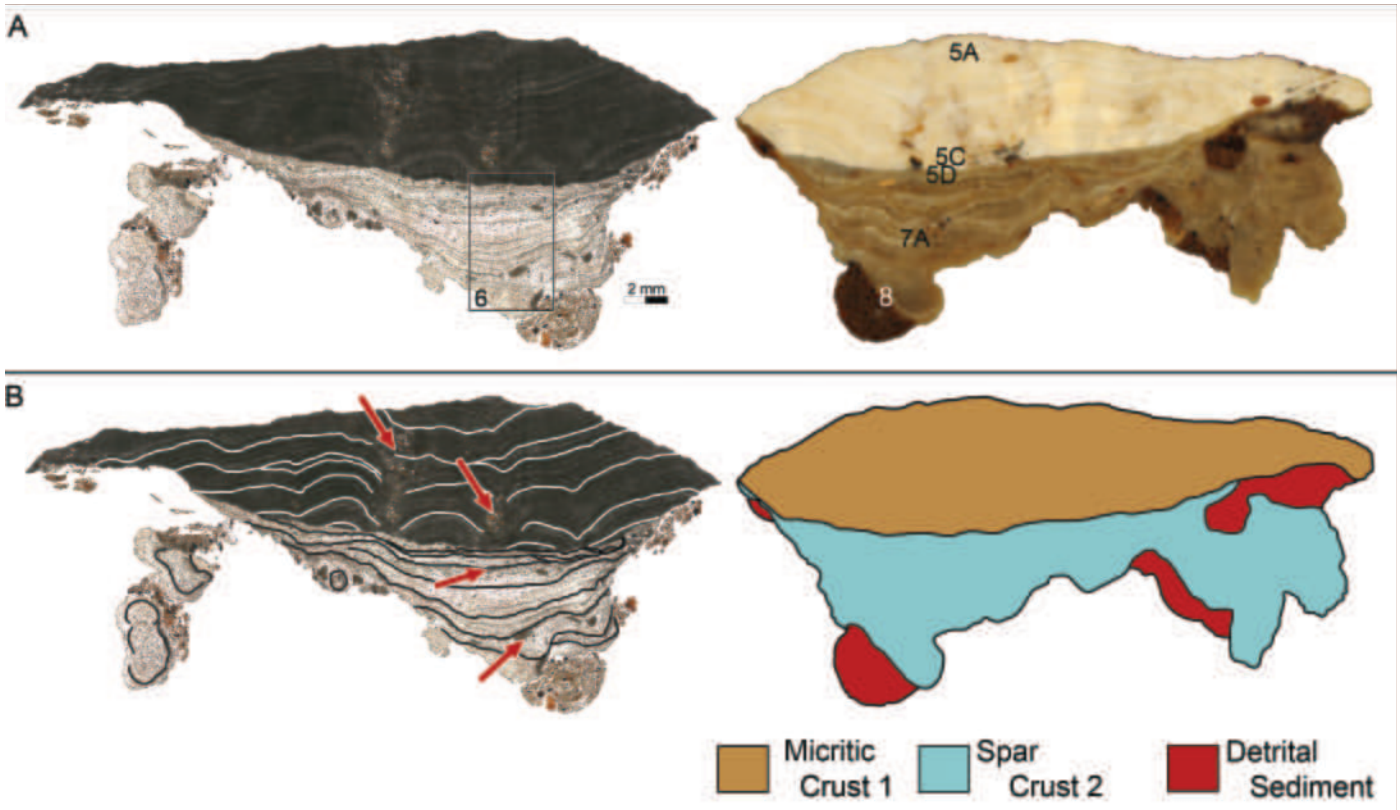

Figure 2. Views of a sample chip of the crust. A: Photomicrograph of a thin section (left) and optical view of the remainer thin section blank (right). These mirror images are separated by the approximately 2 mm thickness of the saw blade. Numbers indicate location of the SEM and optical photomicrographs in Figs. 5, 6, 7, and 8. B left and right: Interpretation of the distribution of the three components from Fig. 2A (right), with growth lines and the distribution of intermixed detrital sediments (red arrows, left and red areas, right). The upper micritic crust (dark color at left, brown at right) grew upward and has been eroded on both the top and the bottom. The lower spar crust (light color at left, blue at right), including the finger-like speleothems, grew downward.

sample, but not all. The low valleys between the domes had depositional relief of up to 2 mm and collected detrital clastic material (quartz silt, clays, and iron oxides; Fig. 2). The laminations are least defined where the clastic material is most abundant.

At higher magnification, the micritic material shows a range of crystal sizes from minimicrite (<1 μm; Folk, 1974) to true micrite (1–5 μm) to microspar (5–20 μm) (Fig. 5A and 5B). Disseminated clay and quartz silt is present in the micrite to minimicrite (Fig. 5A, 5B, and 5C), which contributes to the opaque appearance in plane light (Fig. 2). Patches of microspar sometimes show increased clay between crystals (Fig. 5C).

The laminations are truncated both on top and bottom of the crust (Fig. 2B), indicating erosion of this crust on both sides. The contact between the two crusts is very sharp with large spar crystals nucleating directly on eroded micrite (Figs. 2 and 5D).

Lower Spar Crust

The lower spar crust grew off the eroded underside of the laminated micritic crust and extends as protruding finger-like speleothems (Figs. 2–4, 6). The spar crust is composed of bladed calcite spar with fine downward-curved laminations defined by either thin (1–10 μm) micritic layers or thicker (100–300 μm) micrite with detrital clastics (Fig. 6). Thicker (up to 1 mm) layers include multiple micritic layers and a shift from clear to more yellow spar. The yellow spar has needle molds and fine 1 μm ghost lines when etched for the SEM (Fig. 7A and 7B). The ghost lines are too thin to be seen in thin section (Fig. 6), but they are contained within the spar crystals. Dogtooth crystal terminations are sometimes found buried and preserved by a micritic layer. The bladed calcite crystals nucleate as smaller, equant calcite crystals beneath thicker clastic-rich layers, then they extend through many thin clastic or micritic layers to the next thick clastic-rich layer (Fig. 6A). Quartz silt is scattered throughout the pendant crust, along with rare dolomite silt (Fig. 7A). Rare, ropy, carbon-rich ribbons are present and are associated with detrital material and micrite (Fig. 7C and 7D).

Red-Brown Sediment

The final component is red-brown sediment, partly or wholly detrital, found within and under the pendant crust (Figs. 1 and 2). The sediment is poorly sorted with a clay (silicon-aluminum-magnesium-oxygen) matrix and silt to fine

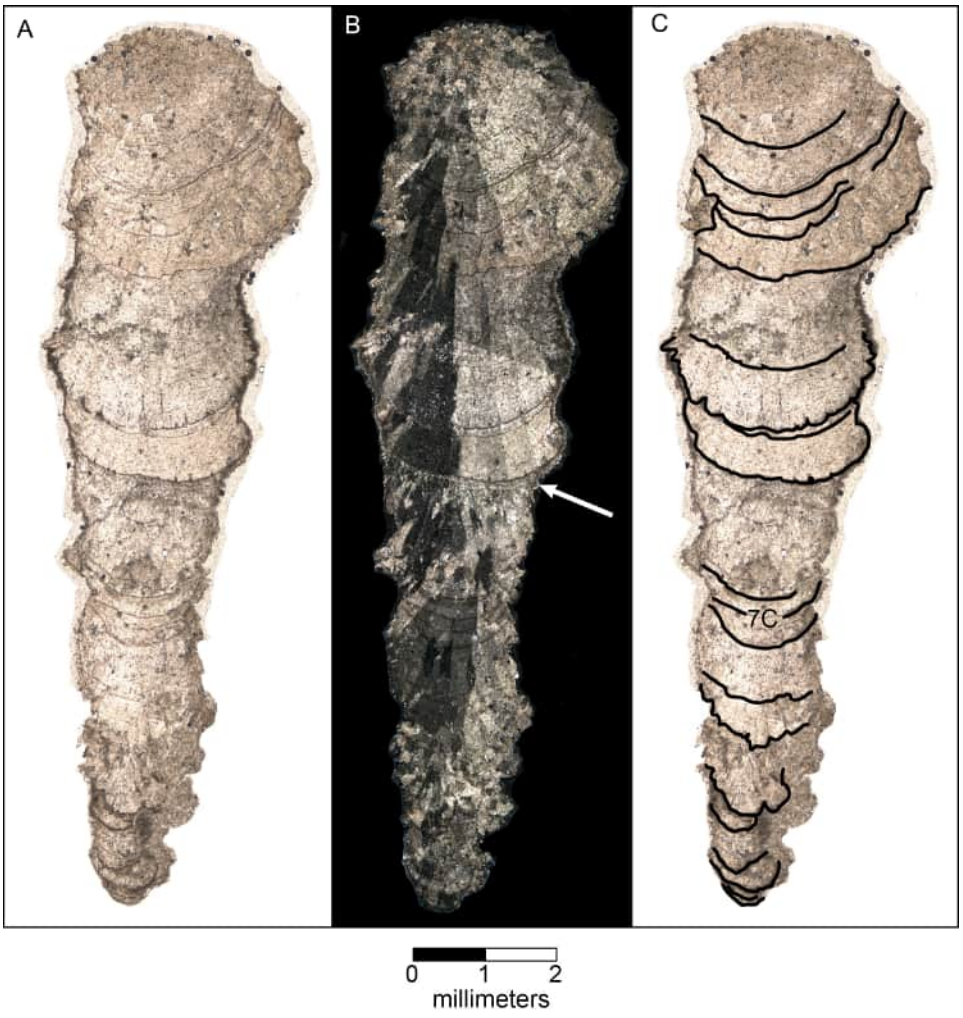

Figure 3. Photomicrographs of a section of a larger, finger-like protrusion. A. Plane-polarized light. B. Cross-polarized light. C. Same as Fig. 3A with black lines interpretating micritic layers showing growth lines and indicating location of Fig. 7C. The protrusion is composed of bladed calcite with detrital inclusions. Bladed crystals extend through many layers. Larger interruptions in growth (e.g., arrow in Fig. 3B) are followed by minor detrital grains and then by renewed calcite growth with new crystals. Note that almost all growth is down with layers oriented perpendicular to growth direction.

sand carbonate (calcite and dolomite), quartz, and iron oxide grains (Figs. 2, 8) as determined by EDS. The disseminated detrital grains in both crusts have the same composition.

DISCUSSION

Interpretation of Fabrics

Micrite in speleothems is increasingly seen as a microbial fabric forming generally during periods of low discharge (Jones, 2009, 2011; Frisia et al., 2012; Frisia, 2015). Stromatolites are microbially laminated structures, most commonly found in shallow, sunlit waters (e.g., Burne and Moore, 1987). However, a number of workers have recognized stromatolites in cave settings in the absence of light (Melim et al., 2001; Gradziński et al., 2010). The upper crust is laminated micrite to microspar, with patches of minimicrite (Figs. 2 and 5) and considerable detrital silt and clays. We interpret this fabric as evidence of stromatolitic growth in a probably subaqueous biofilm, with the detrital material washed in during floods (Fig. 9A). The range of crystal sizes (minimicrite to microspar) with a mottled distribution suggests partial recrystallization, likely from Ostwald ripening (Chai, 1974; Melim and Spilde, 2011, 2021). When formed, the micritic crust was probably continuous to the cave floor, as it appears to coat the floor (Fig. 1B and 1C), and the growth lines are eroded at both the top and bottom of the sample (Fig. 2).

The bladed-calcite spar is interpreted as primary crystal growth based on evidence for nucleation on a substrate, the presence of euhedral crystal terminations (Frisia et al., 2000; Brasier et al., 2011; Melim and Spilde, 2018), and the preservation of growth laminations (Figs. 2–4 and 6). However, the presence of needle molds and ghost laminations (Fig. 7) suggest interruptions in growth and some recrystallization. Needle crystals are indicative of primary aragonite, not calcite. Relatively small changes in the magnesium-calcium ratio of cave waters can lead to aragonite precipitation (Gonzalez and Lohmann, 1988; Riechelmann et al., 2014; Rossi and Lozano, 2016). Aragonite easily recrystallizes to calcite while sometimes preserving crystal relicts (Frisia et al., 2002; Melim and Spilde, 2018). Poorly preserved ghost laminations in cave (mine) pearls formed during recrystallization of very fine (<1 μm) calcite laminations (Melim and Spilde, 2021). We suggest a similar process occurred here.

The internal laminations in the bladed spar indicate pendent growth (Fig. 2). The finger-like protrusions are also generally pendent but often with growth off to one side and rarely even upward (Figs. 1, 3, and 4). Growth, however, is always on the end of the protrusion, not on the sides. This suggests growth from dripping water, rather than while submerged in a cave pool. Since speleothems growing in cave pools are surrounded by water, mineral growth occurs simultaneously in all directions, not just one.

Micritic laminations mark intervals of lesser (or no) spar growth. Based on analogy with stalagmites, micritic intervals likely formed as microbial mats during drier periods (Jones, 2009, 2011; Frisia et al., 2012; Frisia, 2015). The carbon-rich

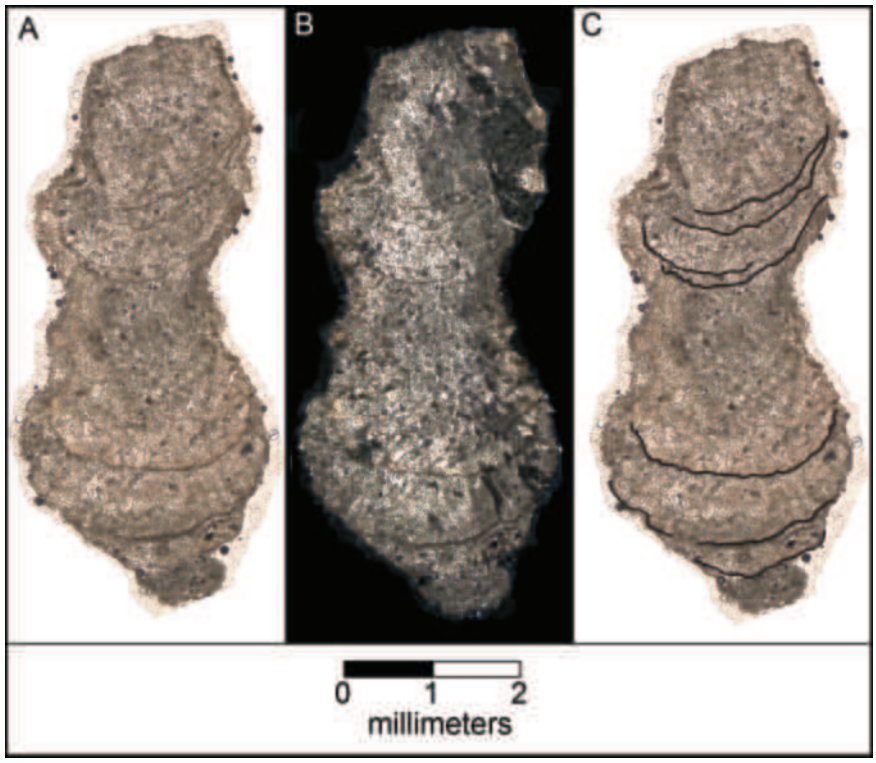

Figure 4. Photomicrographs of a section of a smaller finger-like protrusion. A. Plane-polarized light. B. Cross-polarized light. C. Same as Fig. 4A with black lines interpreting micritic layers showing growth lines. Although bladed calcite crystals are present and extend through many layers, this sample contains more micritic and detrital material. Note that almost all growth is down with layers oriented perpendicular to growth direction.

ribbons are interpreted as preserved biofilm based on the branching, ribbon morphology and carbon-rich composition (e.g., Hofmann et al., 2008; Westall, 2008; Melim et al., 2023). This rare biofilm (Fig. 7C) supports a microbial role.

Detrital material including quartz silt, clays, and carbonate grains washed into the sample area many times during the growth of both crusts (Fig. 2, 3, and 4). In addition, modern sediment partly covers the crust (Fig. 1). During growth of the stromatolitic, micritic crust, the sediment filled in low spots but did not apparently interrupt growth of the microbial biofilm. In contrast, during growth of the pendent crust, larger amounts of detrital material terminated bladed spar crystal growth and formed the substrate for new bladed spar crystals (Figs. 3 and 6).

Origin of Finger-Like Speleothems

Are the Finger-Like Speleothems Helictites or Subaqueous Helictites?

Helictites are speleothems that twist and turn in unpredictable directions, very much like the features here. Davis et al. (1990) proposed an association with gypsum for subaqueous helictites in Lechuguilla Cave, New Mexico. More recently, Tisato et al. (2015) suggested precipitation is associated with biofilms. However, all helictites contain an open central canal (Davis, et al. 1990; Hill and Forti, 1997; Tisato, et al. 2015) that somehow feeds the growing end.

The features here not only lack a central canal, but also the crystal growth patterns indicate there never was a central canal (Figs. 3, 4). Rather, each finger grows along the bottom edge by extension of radiating, bladed calcite. The active surface is the far end, but the entire surface of the end, not just an area around a central canal. Thus, these speleothems are not helictites.

Are the Finger-Like Speleothems Pool Fingers?

Pool fingers are elongate speleothems that extend down from cave walls and shelfstone in cave pools (Davis et al. 1990; Melim et al. 2001, 2009). Pool fingers range from as small as 1–2 mm wide by <1 cm long, up to giant pool fingers 10 cm wide by >1 m long. While many speleothems grow downward in air, where gravity pulls the water down, pool fingers extend down underwater. They are thought to nucleate on microbial filaments or strings of biofilm; continued precipitation of calcite can be either abiologic or further assisted by the biofilm (Davis, et al. 1990; Melim, et al. 2001, 2009). Since pool fingers grow underwater, the mineral growth is continuous on all sides, with the finger growing both down and out. The entire outer surface is active at any one time. Layers along the sides are continuous from the top to the bottom.

Unlike pool fingers, the speleothems from Sistema Los Toros grew in layers extending only at the end of the bladed crystals. Growth lines are curved, but generally perpendicular to the long axis. There is no growth on the sides of higher layers. This suggests they did not grow underwater, but rather grew from dripping water in air.

Are the Finger-Like Speleothems Stalactites?

Stalactites grow as water drips, usually from the ceiling of a cave. Starting as hollow soda straws, growth continues at the end of the central canal and later by flow on the outside (Hill and Forti, 1997). Thus, stalactites grow down but also usually increase in diameter such that larger ones (except soda straws) usually taper downward. Stalactites are commonly composed of radiating fibrous or bladed calcite, much like that seen here, but the growth direction is both down and outward, not just down as here. Finally, stalactites form from actively dripping water, so they seldom curve and they do not branch. Thus, the finger-like speleothems are not stalactites.

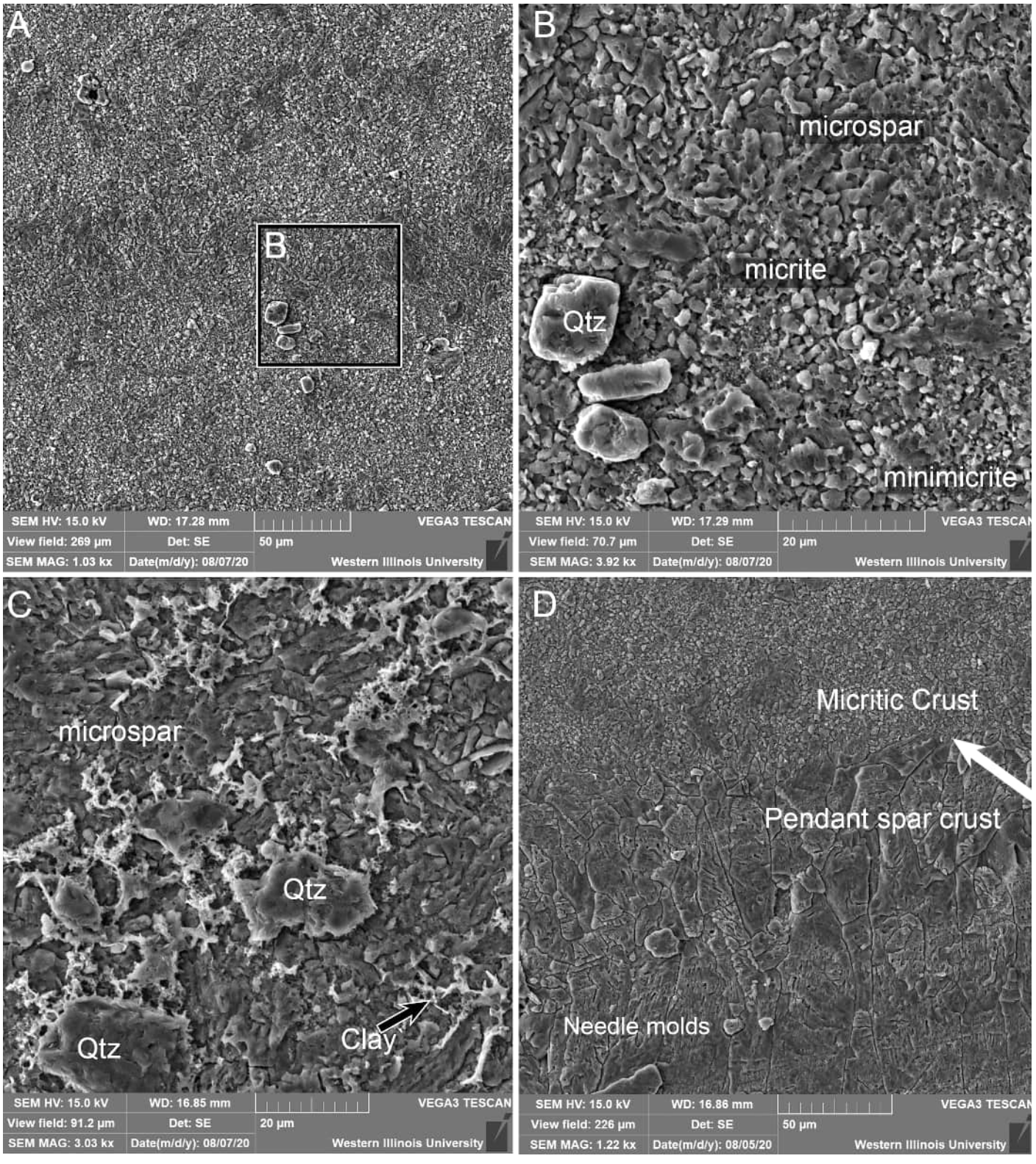

Figure 5. SEM photomicrographs of a section on the upper micritic crust in Fig. 2. Locations of Fig. 5A, 5C, and 5D shown in Fig. 2A (right). A. Typical fabric of micritic crust. B. Detail on micritic crust where shown on Fig. 2A with a range of calcite crystal sizes from minimicrite (<1 µm) to microspar (5–20 µm). Also note quartz silt (Qtz). C. Coarser microspar area with clay minerals concentrated between calcite crystals. Also note quartz silt (Qtz). D. Sharp contact (arrow) between upper micritic crust and lower pendant spar crust. Note etched needle molds within pendant crust (see Figure 7).

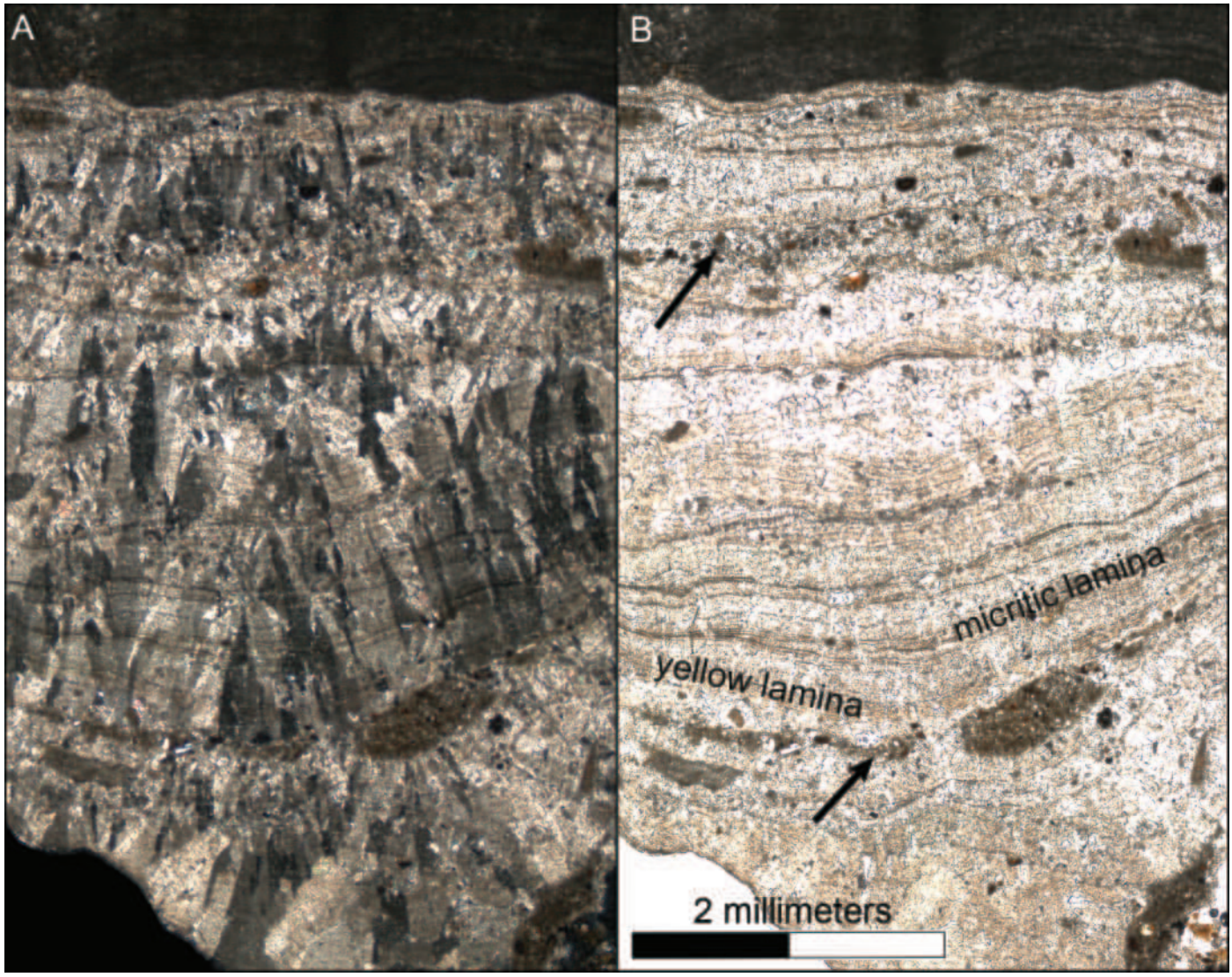

Figure 6. Photomicrographs of a section of the pendant crust. A. Cross-polarized light. B. Plane-polarized light. Thin micritic layers define most laminations but some lack the micrite and are more yellow in color. Bladed calcite crystals nucleate below thicker detrital layers (*arrows*) then coalesce into fewer larger crystals that extend through many layers.

What Are They?

The finger-like speleothems from Sistema Los Toros do not fit any of the existing models for elongate speleothems. They lack the central canal characteristic of helictites even though their irregular and branching form is closest to helictites. Unlike pool fingers, these features grew extending from the end only; thus, the initial diameter is close to the final diameter for most samples. Pool fingers start thin and thicken with time, growing on all sides as well as the end. Stalactites show similar bladed calcite, but differ in that they usually show a central canal and typically taper due to side growth. The crystals radiate outward and downward, rather than just downward as seen here.

For lack of any comparable speleothem, these features are currently unique and we propose the name torosites for them. A brief history of their proposed formation is as follows:

1. A dense, laminated crust grew on an irregular surface (Fig. 9A). Minor loose material washed in, but most of the crust is very fine laminae of micrite, suggesting growth in a biofilm. This crust was hard and lithified, either from the start, or shortly thereafter. In thin section, this crust is dark grey, but it appears white to tan in the cave.
2. The micritic crust was eroded, truncating the growth lines on the top and bottom of the crust and creating a gap beneath the crust (Fig. 9B).
3. A new bladed calcite crust started growing, extending downward from the earlier formed crust and from the cave wall (Fig. 9C). Mostly the bladed calcite grew as pendent, narrow, finger-like speleothems (torosites, Figs. 1, 3, and 4). Growth was mainly along the lower edge of each speleothem, so the torosites generally do not

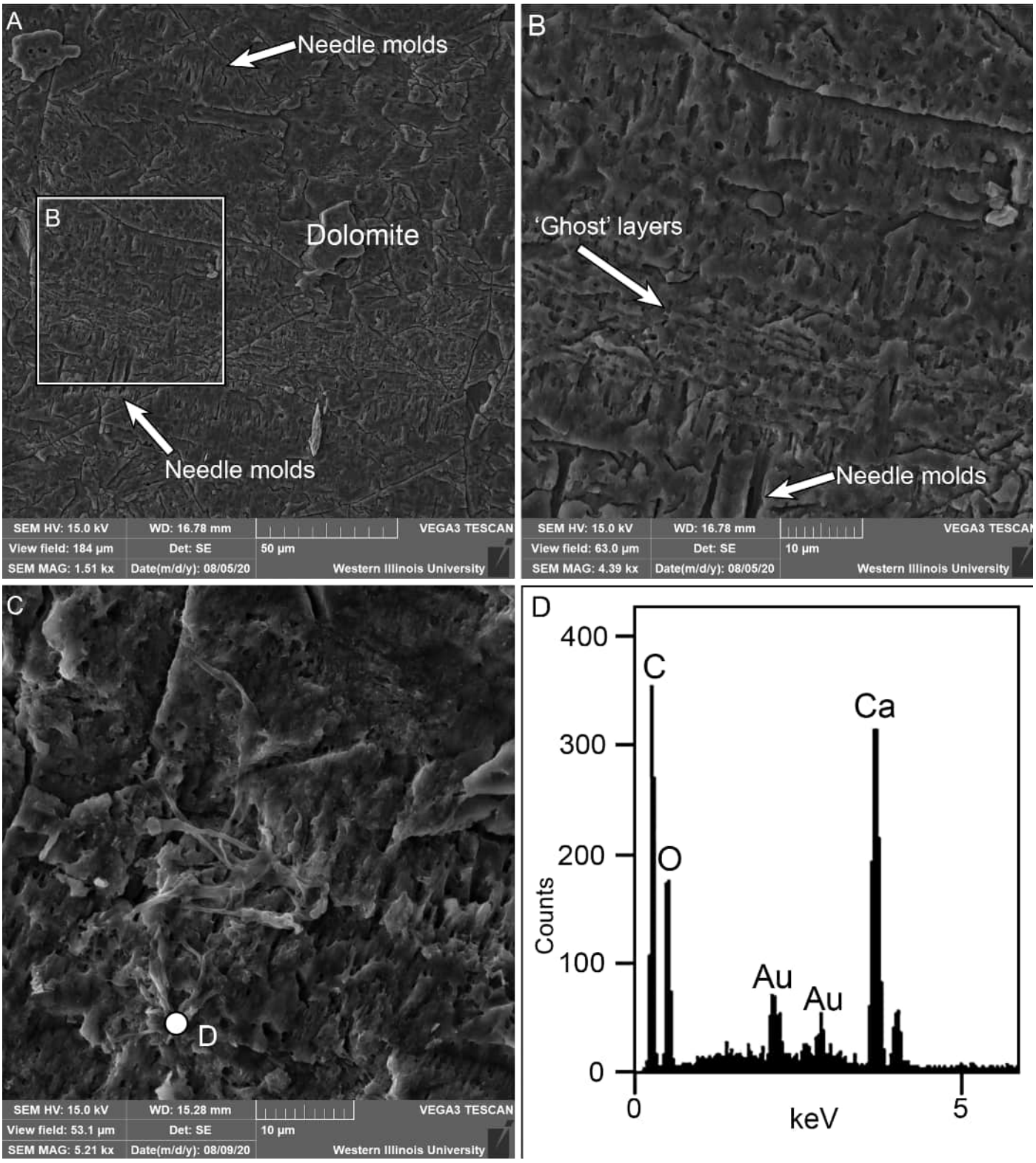

Figure 7. SEM photomicrographs of and EDS spectrum for a section of the pendant spar crust shown in Fig. 2A (right). In thin section these locations are each a single-bladed calcite crystal with faint micritic lamina (see Figs. 2 and 3). A. Typical fabric of the pendant spar crust including needle molds (labeled arrows). Note trace dolomite silt (spectrum not shown). Box is location for Fig. 7B. B. Detail of 1–2 µm ghost layers within the spar crystal in Fig. 7A showing both needle molds and "ghost" layers (labeled arrows). In thin section this location is a single-bladed calcite crystal with faint micritic lamina (see Fig. 2). C. Detail with needle molds and patch of carbon-rich, ropy ribbons, interpreted as biofilm (see text). Dot indicates location for the spectrum in Fig. 7D. D. Energy-dispersive X-ray spectrum of ropy biofilm and the underlying calcite. Adjacent calcium carbonate has a carbon peak that is always less than oxygen (not shown); the much higher carbon peak here indicates additional carbon from the ropy biofilm.

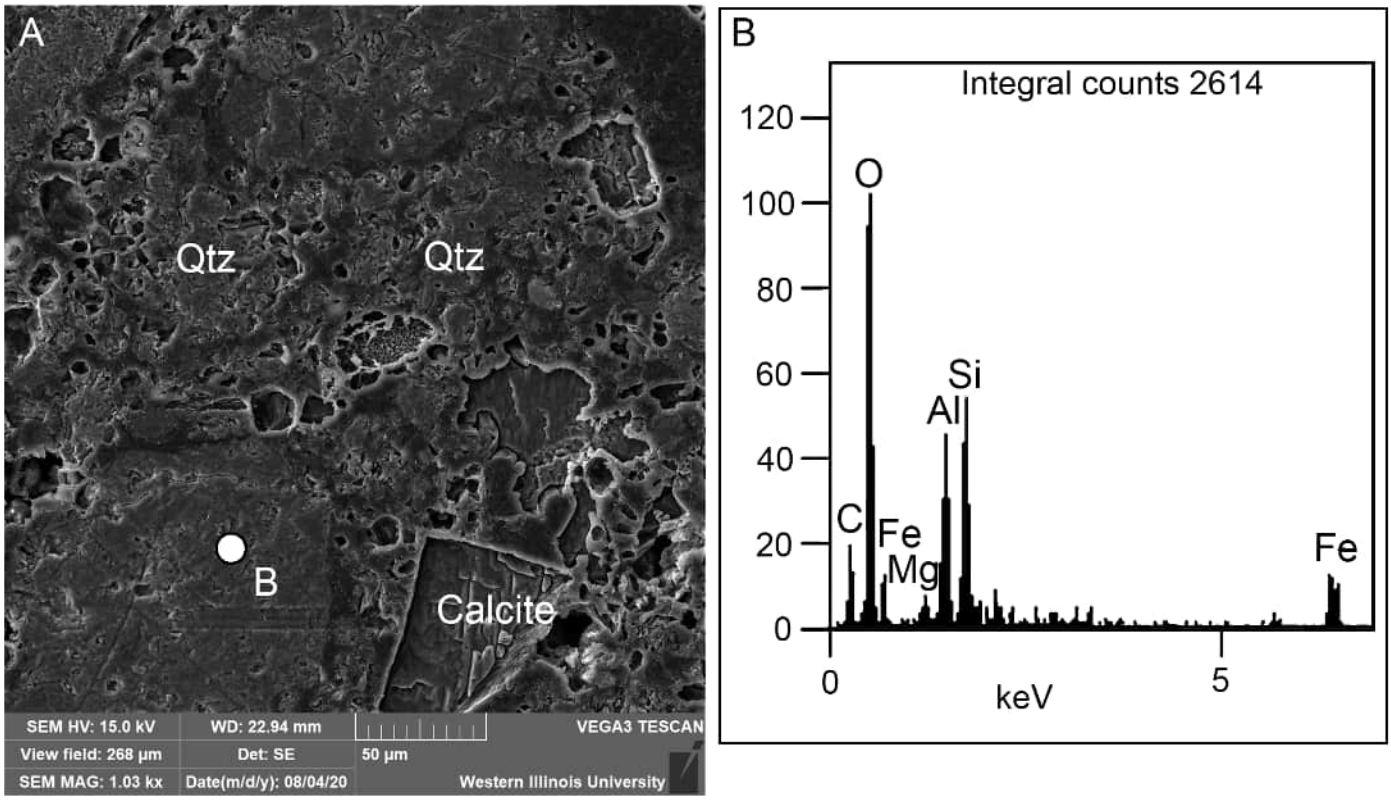

Figure 8. SEM photomicrograph and energy-dispersive X-ray spectrum for the sediment shown in Fig. 2A (right). A. Photomicrograph from etched thin section. Recessive areas are etched carbonate. Grains include quartz (Qtz; spectrum not shown), iron oxides, and clay-rich matrix. Dot indicates location for spectrum in Fig. 8B. B. Energy-dispersive X-ray spectrum at the location on the matrix shown in Fig. 8A. Spectrum shows aluminum-magnesium silicate (clay) and iron oxides. The small carbon peak is likely from the epoxy in the thin section surrounding the clays.

taper. Pauses in growth are indicated by thin, dark layers that include biofilm and detrital grains such as clays and quartz silt. The detrital clays and quartz were washed in from outside, while the calcite grew in place. Thus, a sticky biofilm trapping sediment and precipitating fine calcite formed when conditions were wrong (perhaps too dry) for bladed calcite. When the right conditions returned, bladed calcite resumed extending existing crystals or started over when the crust was too thick. Some recrystallization of the bladed spar is suggested by the presence of molds indicating former aragonite and very fine ghost laminations indicating finer laminations lost to recrystallization.

4. Based on the red-brown sediment surrounding the torosites (Fig. 2), this area was partly or completely buried with cave sediment (Fig. 9D). This burial may have terminated growth or may have happened some time after growth stopped for another, unknown reason. This sediment is much greater volume than the minor detrital material within the earlier carbonate crusts.
5. The current setting appears to be one of erosion having removed the red-brown sediment and exhuming the earlier-formed speleothems.

The most puzzling aspect of torosites is their irregular growth, often sideways or even upward instead of just downward as predicted for growth in dripping water. We speculate that the irregular direction of new growth is somehow related to the presence of the microbial biofilm. Tisato et al. (2015) proposed a similar origin for curving helictites in Asperge Cave in France. They identified a complex microbial community on their living examples, but could not determine what aspect of the living biofilm caused the irregular growth. They suggest preferential growth by the microbial community toward lesser mineralization, or greater humidity or air currents, or simply random growth (Tisato et al., 2015). The torosites preferentially grow outward from each peninsula (Fig. 1D), so perhaps higher air flow is influencing microbial growth.

SIGNIFICANCE

Speleothems come in an amazing array of forms (Hill and Forti, 1997). Once thought to be largely abiotic, many workers are now recognizing a microbial component (e.g., Jones, 2001, 2010; Fairchild and Baker, 2012). In some speleothems, there is even a growing recognition for major role for microbes, including in moonmilk (Bindschedler, et al., 2014; Cacchio,

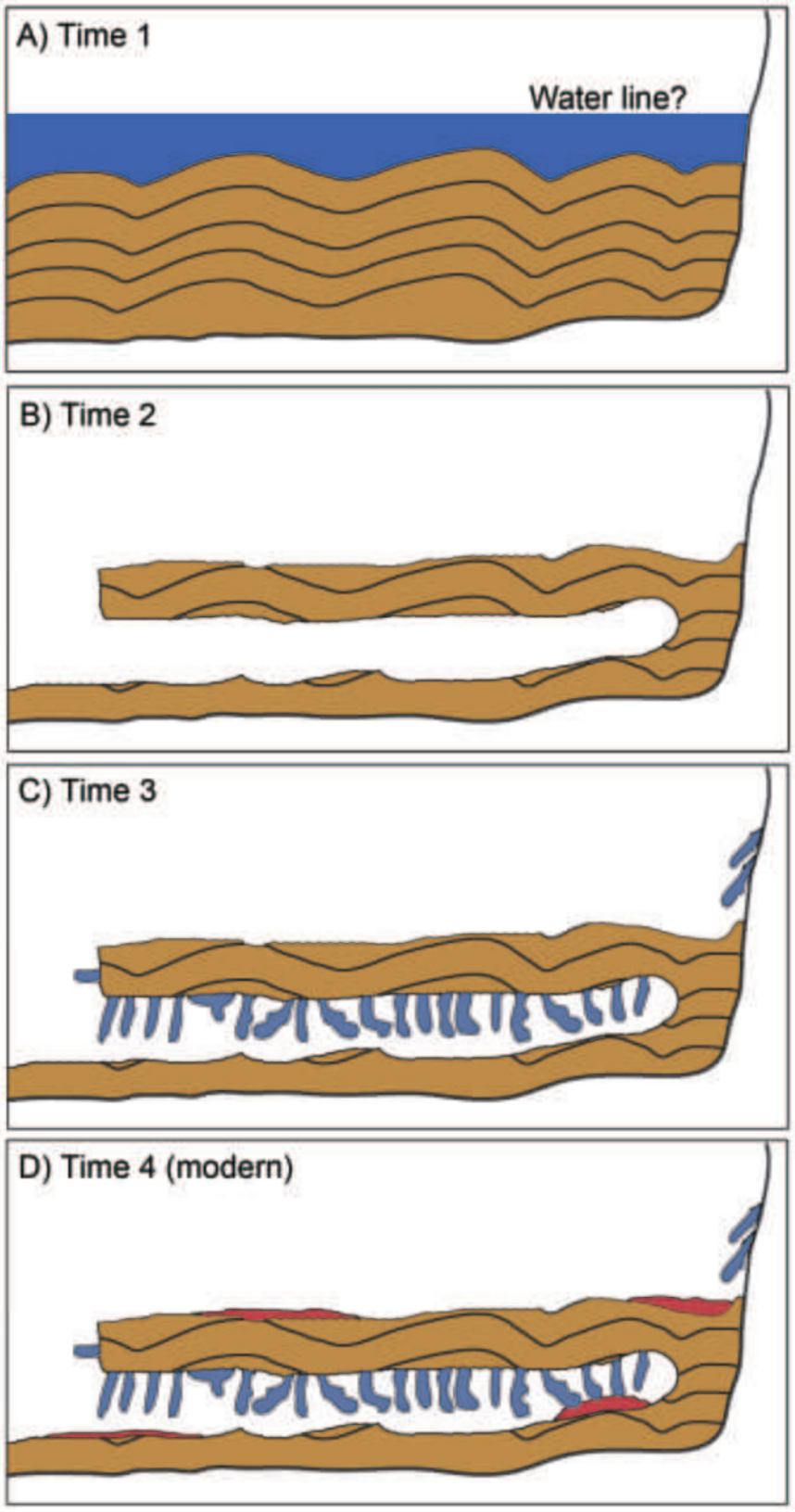

Figure 9. Model for development of the research site. A. Time 1: Formation of the micritic crust as a stromatolite, likely under water, but possibly with flowing water at times. B. Time 2: Erosion of the micritic crust, leaving truncated growth lines on the top and bottom. C. Time 3: Growth of the spar crust and finger-like protrusions, mainly on the base of the micritic crust but also on the wall above. D. Time 4: Modern detrital sediment partly covering both crusts.

et al. 2014), pool fingers (Davis, et al., 1990; Melim et al., 2001, 2009), some cave pearls (Jones and MacDonald, 1989; Jones, 2009; Melim and Spilde, 2018), some helictites (Tisato, et al. 2015), and hells bells (Stinnesbeck et al., 2018; Ritter et al., 2019). Although the details vary, all of these features are now thought to depend on the presence of microbial biofilms to produce the distinct morphology; so each is microbially mediated, rather than just including the presence of microbes (Jones, 2001). The irregular growth pattern of torosites is best explained as a result of microbial biofilms influencing the direction of growth. Thus, torosites add another example to this growing list of microbially mediated speleothems.

CONCLUSIONS

We interpret irregular, finger-like protrusions extending down from the base and edges of a micritic crust in Sistema Los Toros, Nuevo Léon, Mexico, as unique, microbially mediated speleothems, torosites, based on the following:

a. Torosites grow down and outward from beneath an eroded micritic crust and off the cave wall.

b. Each finger-like protrusion thickens and thins, but maintains about the same 2–3 mm width, giving an appearance like a finger with swollen knuckles.

c. They are composed of bladed spar with micritic and detrital laminations, much like many stalactites, but they lack any central canal.

d. Unlike pool fingers and stalactites, they grow on the end only, not along the sides.

We interpret this as growth from slowly dripping water, enough to produce a drop on the end but not enough to precipitate calcite along the sides. Growth was at least partly in a biofilm, which likely contributed to the irregular growth direction of the torosites.

REFERENCES

Bindschedler, S., Cailleau, G., Braissant, O., Millière, L., Job, D., and Verrecchia, E.P., 2014, Unravelling the enigmatic origin of calcitic nanofibres in soils and caves: Purely physicochemical or biogenic processes? Biogeosciences, v. 11, p. 2809–2825, https://doi.org/10.5194/bg-11-2809-2014.

Brasier, A.T., Andrews, J.E., and Kendall, A.C., 2011, Diagenesis or dire genesis? The origin of columnar spar in tufa stromatolites of central Greece and the role of chironomid larvae: Sedimentology, v. 58, p. 1283–1302, https://doi.org/10.1111/j.1365-3091.2010.01208.x.

Burne, R.V., and Moore, L.S., 1987, Microbialites: Organosedimentary deposits of benthic microbial communities: PALIAOS, v. 2, p. 241–254, https://doi.org/10.2307/3514674.

Cacchio, P., Ferrini, G., Ercole, C., Del Gallo, M., and Lepidi, A., 2014, Biogenicity and characterization of moonmilk in the Grotta Nera (Majella National Park, Abruzzi, central Italy): Journal of Cave and Karst Studies, v. 76, p. 88–103, https://doi.org/10.4311/2012MB0275.

Chai, B.H.T., 1974, Mass transfer of calcite during hydrothermal recrystallization, *in* Hoffman, A.W., Giletti, B.J., Yoder, H. S., Jr., and Yund, R.A., eds., Geochemical Transport and Kinetics: Washington, Carnegie Institution of Washington, p. 205–218, https://publicationsonline.carnegiescience.edu/publications_online/geochemical_transport_kinetics.pdf.

Davis, D.G., Palmer, M.V., and Palmer, A.N., 1990, Extraordinary subaqueous speleothems in Lechuguilla Cave, New Mexico: NSS Bulletin, v. 52, p. 70–86.

Fairchild, I.J., and Baker, A., 2012, Speleothem Science: From Process to Past Environments, Oxford, Wiley-Blackwell, 432 p., https://doi.org/10.1002/9781444361094.

Folk, R.L., 1974, The natural history of crystalline calcium carbonate: Effect of magnesium content and salinity: Journal of Sedimentary Petrology, v. 44, p. 141–153, https://doi.org/10.1306/74D72973-2B21-11D7-8648000102C1865D.

Frisia, S., 2015, Microstratigraphic logging of calcite fabrics in speleothems as tool for paleoclimate studies: International Journal of Speleology, v. 44, p. 1–16, https://digitalcommons.usf.edu/ijs/vol44/iss1/1/.

Frisia, S., Borsato, A., Fairchild, I.J., McDermott, F., and Selmo, E.M., 2002, Aragonite-calcite relationships in speleothems (Grotte de Clamouse, France): Environment, fabrics, and carbonate geochemistry: Journal of Sedimentary Research, v. 72, p. 687–699, https://doi.org/10.1306/020702720687.

Frisia, S., Borsato, A., Fairchild, I.J., and McDermott, F., 2000, Calcite fabrics, growth mechanisms, and environments of formation in speleothems from the Italian Alps and southwestern Ireland: Journal of Sedimentary Research, v. 70, p. 1183–1196, https://doi.org/10.1306/022900701183.

Frisia, S., Borsato, A., Drysdale, R.N., Paul, B., Greig, A., and Cotte, M., 2012, A re-evaluation of the palaeoclimatic significance of phosphorus variability in speleothems revealed by high-resolution synchrotron micro XRF mapping: Climate of the Past, v. 8, p. 2039–2051, https://doi.org/10.5194/cp-8-2039-2012.

Gonzalez, L.A., and Lohmann, K.C., 1988, Controls on mineralogy and composition of spelean carbonates: Carlsbad Caverns, New Mexico, *in* James, N.P., and Choquette, P.W., eds., Paleokarst: New York, Springer-Verlag, p. 81–101, https://doi.org/10.1007/978-1-4612-3748-8_4.

Gradziński, M., Chmiel, M.J., Lewandowska, A., and Michalska-Kasperkiewicz, B., 2010, Siliciclastic microstromatolites in a sandstone cave: Role of trapping and binding of detrital particles in formation of cave deposits: Annales Societatis Geologorum Poloniae, v. 80, p. 303–314, http://asgp.pl/sites/default/files/volumes/80_3_303_314.pdf.

Hill, C.A., and Forti, P., 1997, Cave Minerals of the World, 2nd ed., Huntsville, Alabama, National Speleological Society, 463 p.

Hofmann, B.A., Farmer, J.D., von Blanckenburg, F., and Fallick, A.E., 2008, Subsurface filamentous fabrics: An evaluation of origins based on morphological and geochemical criteria, with implications for exopaleontology: Astrobiology, v. 8, p. 87–117, https://doi.org/10.1089/ast.2007.0130.

Jones, B., 2001, Microbial activity in caves—a geological perspective: Geomicrobiology Journal, v. 18, p. 345–358, https://doi.org/10.1080/01490450152467831.

Jones, B., 2009, Cave pearls—the integrated product of abiogenic and biogenic processes: Journal of Sedimentary Research, v. 79, p. 689–710, https://doi.org/10.2110/jsr.2009.071.

Jones, B., 2010, Microbes in caves: Agents of calcite corrosion and precipitation, *in* Pedley, H.M., and Rogerson, M., eds., Tufas and Speleothems: Unravelling the Microbial and Physical Controls, special publication 336: London, Geological Society, p. 7–30, https://doi.org/10.1144/SP336.2.

Jones, B., 2011, Stalactite growth mediated by biofilms: Example from Nano Cave, Cayman Brac, British West Indies: Journal of Sedimentary Research, v. 81, p. 322–338, https://doi.org/10.2110/jsr.2011.28.

Jones, B., and MacDonald, R.W., 1989, Micro-organisms and crystal fabrics in cave pisoliths from Grand Cayman, British West Indies: Journal of Sedimentary Petrology, v. 59, p. 387–396, https://doi.org/10.1306/212F8F9E-2B24-11D7-8648000102C1865D.

Melim, L.A., Liesheidt, R., Northup, D.E., Spilde, M.N., Boston, P.J., and Queen, J.M., 2009, A biosignature suite from cave pool precipitates, Cottonwood Cave, New Mexico: Astrobiology, v. 9, p. 907–917, https://doi.org/10.1089/ast.2009.0345.

Melim, L.A., Mure-Ravaud, S.R., Hegna, T.A., Bellott, B.J., and Lerosey-Aubril, R., 2023, Silicification of trilobites and biofilm from the Cambrian Weeks Formation, Utah: Evidence for microbial mediation of silicification: Geology, v. 51, p. 80–84, https://doi.org/10.1130/G50496.1.

Melim, L.A., Shinglman, K.M., Boston, P.J., Northup, D.E., Spilde, M.N., and Queen, J.M., 2001, Evidence of microbial involvement in pool finger precipitation, Hidden Cave, New Mexico: Geomicrobiology Journal, v. 18, p. 311–330, https://doi.org/10.1080/01490450152467813.

Melim, L.A., Northup, D.E., Boston, P.J., and Spilde, M.N., 2016, Preservation of fossil microbes and biofilm in cave pool carbonates and comparison to other microbial carbonate environments: PALAIOS, v. 31, p. 177–189, https://doi.org/10.2110/palo.2015.033.

Melim, L.A., and Spilde, M.N., 2011, Rapid growth and recrystallization of cave pearls in an underground limestone mine: Journal of Sedimentary Research, v. 81, p. 775–786, https://doi.org/10.2110/jsr.2011.65.

Melim, L.A., and Spilde, M.N., 2018, A new unified model for cave pearls: Insights from cave pearls in Carlsbad Cavern, New Mexico, U.S.A: Journal of Sedimentary Research, v. 88, p. 344–364, https://doi.org/10.2110/jsr.2018.21.

Melim, L.A., and Spilde, M.N., 2021, The rise and fall of cave pearl pools: Highly variable growth, recrystallization, and demise of a mine pearl site: Sedimentology, v. 68, p. 2165–2194, https://doi.org/10.1111/sed.12848.

National Institutes of Health, 2021, ImageJ: Image processing and analysis in Java, software version 1.53k, https://imagej.net/ij/download/src/.

Riechelmann, S., Schröder-Ritzrau, A., Wassenburg, J.A., Schreuer, J., Richter, D.K., Riechelmann, D.F.C., Terente, M., Constantin, S., Mangini, A., and Immenhauser, A., 2014, Physicochemical characteristics of drip waters: Influence on mineralogy and crystal morphology of recent cave carbonate precipitates: Geochimica et Cosmochimica Acta, v. 145, p. 13–29, https://doi.org/10.1016/j.gca.2014.09.019.

Ritter, S.M., Isenbeck-Schröter, M., Scholz, C., Keppler, F., Gescher, J., Klose, L., Schorndorf, N., Avilés Olguín, J., González-González, A., and Stinnesbeck, W., 2019, Subaqueous speleothems (hells bells) formed by the interplay of pelagic redoxcline biogeochemistry and specific hydraulic conditions in the El Zapote sinkhole, Yucatán Peninsula, Mexico: Biogeosciences, v. 16, p. 2285–2305, https://doi.org/10.5194/bg-16-2285-2019.

Rossi, C., and Lozano, R.P., 2016, Hydrochemical controls on aragonite versus calcite precipitation in cave dripwaters: Geochimica et Cosmochimica Acta, v. 192, p. 70–96, https://doi.org/10.1016/j.gca.2016.07.021.

Stinnesbeck, W., et al., 2018, Hells bells – unique speleothems from the Yucatán Peninsula, Mexico, generated under highly specific subaquatic conditions: Palaeogeography, Palaeoclimatology, Palaeoecology, v. 489, p. 209–229, https://doi.org/10.1016/j.palaeo.2017.10.012.

Tisato, N., et al., 2015, Microbial mediation of complex subterranean mineral structures: Scientific Reports, v. 5, p. 15525, https://doi.org/10.1038/srep15525.

Westall, F., 2008, Morphological biosignatures in early terrestrial and extraterrestrial materials: Space Science Reviews, v. 135, p. 95–114, https://doi.org/10.1007/s11214-008-9354-z.